Developing Microelectrode Arrays for the Point-of-Care Multiplex-Detection of Metabolites

Yu-Chia Chang, Benoit Arnould, Jen Heemstra, and Kevin D. Moeller*

Department of Chemistry, Washington University in St. Louis, St. Louis, MO 63130 USA

Abstract: DNA-aptamer functionalized electrode arrays can provide an intriguing method for detecting pathogen derived exometabolites. This work addresses the limitations of previous aptamer-based pathogen detection methods by introducing a novel surface design that bridges the gap between initial efforts in the area and the demands of a point-of-care device. Specifically, the use of a diblock copolymer coating on a high-density microelectrode array and Cu-mediated cross coupling reactions that allow for the exclusive functionalization of that coating by any electrode or set of electrodes in the array provides a device that is stable for a year and compatible with the multiplex detection of small-molecule targets. The new chemistry developed allows one to take advantage of a large number of electrodes in the array with one experiment described herein capitalizing on the use of 960 individually addressable electrodes.

Introduction

With the developing crisis associated with antibiotic resistance,[1-3*] we have a critical need for both new families of antibiotics and new "point-of-care" diagnostics that allow physicians to make informed decisions about when those antibiotics should be used. In this effort, microelectrode arrays have the potential to provide a platform for developing the "point-of-care" diagnostics needed.[4-6] In principle, microelectrode arrays can be employed to detect multiple metabolites generated by a pathogen in real-time using a library of molecular recognition elements (Figure 1, A and B). These metabolites can be used to characterize the pathogen and assess its risk to the patient.[7-10] The method is inexpensive, fast, and compatible with applications at remote, point-of-care locations. Since the metabolites generated by a pathogen provide a footprint of its activity and potential danger, their rapid identification can be key to making decisions about whether an antibiotic is needed.

Central to the method is the placement of unique molecular recognition elements by individually addressable electrodes in the array. The array is then inserted into a solution that contains any potential metabolites that might be present and an added redox mediator. A sufficiently large potential difference is then set between the array and a remote electrode to induce a current involving the redox mediator at every electrode in the array. This current is generated by either oxidation of the redox mediator at the array and re-reduction at the remote counter electrode, or reduction of the redox

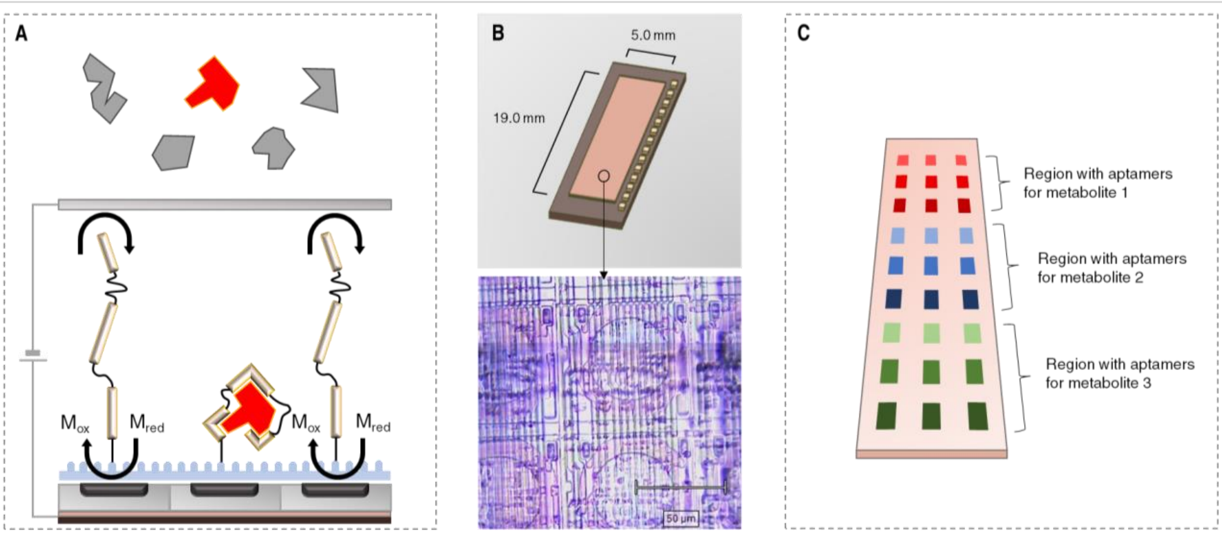

Figure 1. Microelectrode array and a plan for metabolite detection. (**A**) Aptamers on a microelectrode array interact with targeted metabolites and alter the current associated with a redox mediator. (**B**) The dimension of a microelectrode array and its image under microscope. (**C**) A plan for an array.

mediator at the array and re-oxidation at the remote electrode. When a binding event occurs between a molecular recognition element on the array and a metabolite in the solution, it alters this current at the associated electrodes. That change in current can be quantified and recorded.

A number of groups have pioneered the use of DNA-aptamers as the molecular recognition element for this experiment. Seminal work in the area was done by the Barton,[11] Francis,[12] and Plaxco groups,[13] with the Furst group recently adding nicely to this effort.[14] However, for the specific application proposed here, there is an underlying problem with the approaches taken to date. All diagnostic devices contain three main features; a molecular recognition event that detects a target, a device that monitors, records, and quantifies that event, and a surface that connects the two. The surface plays a critical role in the experiment, and its long-term stability and compatibility with the chemistry needed for both construction of the device and the subsequent signaling experiment can represent a significant barrier to the construction and application of a point-of-care device. Current efforts to capitalize on aptamer based electrochemical devices have typically used thiol-based self-assembled monolayers (SAMs) for this surface.[15] The surfaces offer great advantages in terms of signaling experiments because mediators can reach the electrodes easily, and they are compatible with direct detection approaches where a redox reporter is incorporated into the aptamer.[13,14] However, thiol-based SAMs lack the stability needed for a long-term applications, with the most stable SAMs surviving for around a month.[16] Recently, a more stable Se-based SAM has been reported on a gold electrode.[17] The stability of this SAM is derived from the strength of the Se-Au interaction. While one can imagine utilizing Se-based SAMs in the future, most commercial high density microelectrode arrays that contain the number of electrodes needed for the proposed experiments (see below) are made with Pt-electrodes, and the bonding of selenium to platinum surfaces has not been defined in the manner that the Se-Au surfaces have been Since the goal was to develop a general strategy that is available to anyone, the new surfaces developed sought to take advantage of the commercially available Pt-based platform with existing chemistry. In that regard, it is also important to note that a thiol- or a Se-based SAM would react with a wide range of chemical reagents and reactions. This limits the methods that can be used to modify an electrode surface to a small subset of the synthetic chemistry toolbox. One needs to avoid oxidants like Cu(II), a reagent that will play a key role in chemistry developed below. As a result of these limitations, the aptamer-based methods described to date use a minimal number of electrodes to examine the interaction between one aptamer and one metabolite at a time.

This is a significant problem for the planned application highlighted in Figure 1. The selective identification of an infectious pathogen requires the detection and quantification of a family of metabolites in urine. In such cases, it is best if more than one molecular recognition element is used to make a positive identification for each metabolite in order to avoid a false positive signal that might arise from any one molecular recognition element. Hence, a diagnostic device for pathogen characterization requires the use of multiple aptamers targeting multiple metabolites. As an example, a plan is forwarded in Figure 1C for an array that would target three metabolites with three aptamers each. The aptamers would be placed on the array in triplicate to aid with statistical analysis. In addition, it would be best if each block of electrodes (indicated by the colored rectangles) used to support one of the aptamers used more than one electrode. For the proposed experiments, 20 individual electrodes were used for each block in the picture so a faulty electrode would only reduce the total current measured for the block of electrodes by around 5%. With this in mind, the strategy proposed for identifying three metabolites with three aptamers each would utilize 540 electrodes in the array. An expansion of the method to identify 4 metabolites with three aptamers each would utilize 720 electrodes in the array. The construction and analysis of these more complex libraries of aptamers is not compatible with the use of a SAM as the surface on the array, especially if the array is to be used at a remote point-of-care location long after the library is synthesized.

Experimental Section

Materials

The 5'-hexynyl and 3′-6-FAM (Fluorescein)- modified aptamers were purchased from Integrated DNA Technologies, Inc. (Coralville, IA) and used without further purification. The aptamer sequences are listed in Table S1. The bis(pinacol) diboron substrate was purchased from Matrix, Inc. (Columbia, SC). Other materials were purchased from Sigma-Aldrich (St. Louis, MO) and used as received unless otherwise noted.

Instrumentation for microelectrode array experiments

A microelectrode array with a density of 12,544 electrodes • cm^{-2}, provided by CustomArray, Inc. (Bothell, WA), was employed for our experiments. We utilized the ElectraSense reader, manufactured by CustomArray, Inc., to carry out the reactions on the array. To activate specific electrodes on the array for our analytical studies, we utilized the ElectraSense reader, and controlled the potential sweep using an external BAS 100B Electrochemical Analyzer.

Fluorescent studies on microelectrode arrays

For the quantitative fluorescence microscopy, we examined the array using a Nikon Eclipse E200 microscope equipped with an X-Cite 120Q lamp illuminator and a Nikon D5000 camera. Optical filters used were as follows: ET-GFP (FITC/Cy2) (Chroma) filter cube excitation 450-490 nm, emission 500-550 nm, TxRed-A-

Basic-000 (Semrock) filter cube excitation 540-580 nm/emission 590-670 nm, and CFW-BP01-Clinical-000 (Semrock) filter cube excitation 380-395 nm/emission 420-470 nm were employed as optical filters. Fluorescence data were quantitatively analyzed using ImageJ.

General procedure for performing synthetic reactions on the microelectrode array

Detailed procedures for polymer coating on arrays are provided in the Supporting Information. Following the coating, the aryl bromide polymer surface of the microelectrode array was converted to a borate ester surface. This conversion was carried out in 105 µL of a solution containing bis(pinacolato)diboron, tetrabutylammonium bromide, copper sulfate, triphenylphosphine, and a 7:2:1 mixture of acetonitrile, DMF, and water. The desired electrode region was turned on and set at a potential of -1.7 V relative to the Pt-cap for 90 s. The reaction was repeated four times. The microelectrode array was washed with ethanol and dried following the reaction. Then, the array was then immersed in the solution mixture containing the desired ligand and electrolyte, and an oxidation reaction was performed by setting selected electrodes in the array to a potential of +2.0V relative to the Pt-cathode in the cap for the flow cell for 20 cycles (30 s on and 10s off). The array was washed with ethanol following the reaction.

General procedure for analytical measurement on the microelectrode array

Electrochemical evaluation of small molecules and their aptamers binding was accomplished by cyclic voltammetry. The array was secured on an ElectraSense reader, and the flow cell was filled with the mediator solution. The mediator solution contained 8 mM quinone and benzoquinone redox couple in PBS. Electrochemical measurements were recorded from +400mV to -700mV relative to the counter electrode. All peak currents were calculated by BAS 100W Ver 2.31 and plotted by Origin Pro 9 64-bit. The peak current at the selected electrode was obtained by calculating the difference between the current at the oxidative wave and the reductive wave. Calibration curves of peak current vs small molecule concentration were plotted using GraphPad Prism 6. Each data point represents the average of the peak current measured for four 5x4 blocks of electrodes, and the error bars show standard deviation.

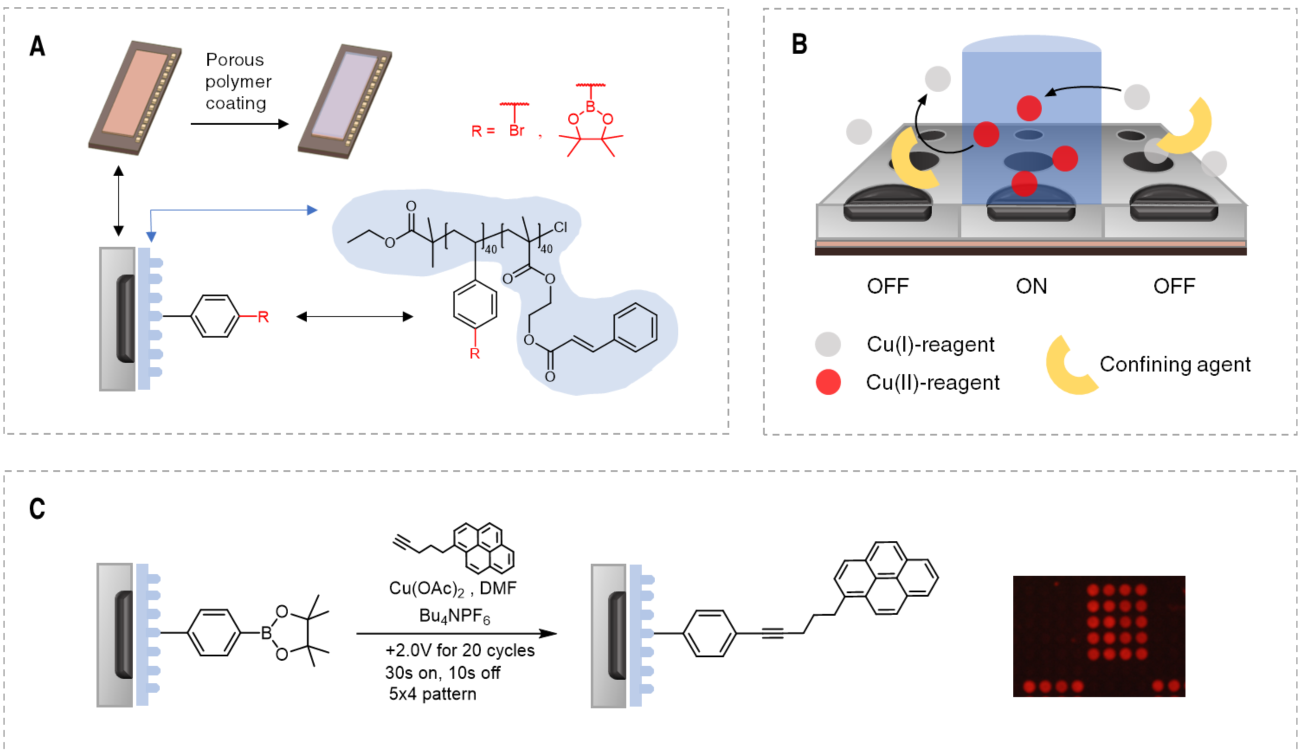

Figure 2. A diblock copolymer for building a porous reaction layer on a microelectrode array. (**A**) Structure of the diblock copolymer. (**B**) The approach used for site-selective chemistry on an array. The reagent needed for the reaction, Cu(II), is generated at the selected electrode by a oxidation of Cu(I). A "confining agent" that reacts with the Cu(II) and reduces it to Cu(I) is added to the solution above the array so that the Cu(II) cannot migrate to electrodes not selected for the reaction. (**C**) An example highlighting a Cu(II)-mediated Chan-Lam coupling reaction. In this case, excess acetylene is used in solution as the confining agent.

Results and Discussion

Compatibility of a new surface with signaling: With these issues in mind, we turned to a more stable diblock copolymer surface for the arrays (Figure 2A).[18,19] The polymer contained one block functionalized with a cinnamate ester that could be photodimerized to add stability to a surface, and a second block that contained either an arylbromide or an arylborate moiety so that molecules could be added to the surface of an electrode in the array. Both blocks were comprised of around 40 monomers. The polymer was spin-coated onto an array, and then the surface photo-crosslinked.

Previously developed methods for selectivity functionalizing the polymer surface on the array by selected electrodes in the array focused on the use of indirect electrochemical methods. The overall synthetic approach (highlighted in Figure 2B) utilizes selected electrodes in the array to convert a pre-catalyst or reagent into the catalyst or reagent needed for a desired transformation on the polymer.[20,21] A "confining agent" is added to the solution above the array in order to destroy any catalyst or reagent that migrates away from the electrode used for its generation. In this way, the reaction only occurs at the selected electrodes.

A specific example of this exact approach is shown in Figure 2C. The array was treated with a solution that contained a Cu(I)-reagent, and then selected electrodes in the array (blocks of 12 electrodes each) used as anodes to oxidize the Cu(I)-reagent to form a Cu(II)-species and mediate a Chan-Lam coupling reaction between an acetylene in solution and an arylborate substrate on the surface of the electrode.[22] The Cu(II)-species, which would not be compatible with the use of an oxidation-sensitive thiol-based surface, was confined to the selected electrodes in the array with the use of excess acetylene substrate in solution. Cu(II)-reagents serve as oxidants for the dimerization of these end-chain acetylenes, a process that reduces two equivalents of Cu(II) to two equivalents of Cu(I). This solution phase reduction of Cu(II) reverses the oxidation reaction that took place at the electrode in order to make the Cu(II). By controlling the relative rates

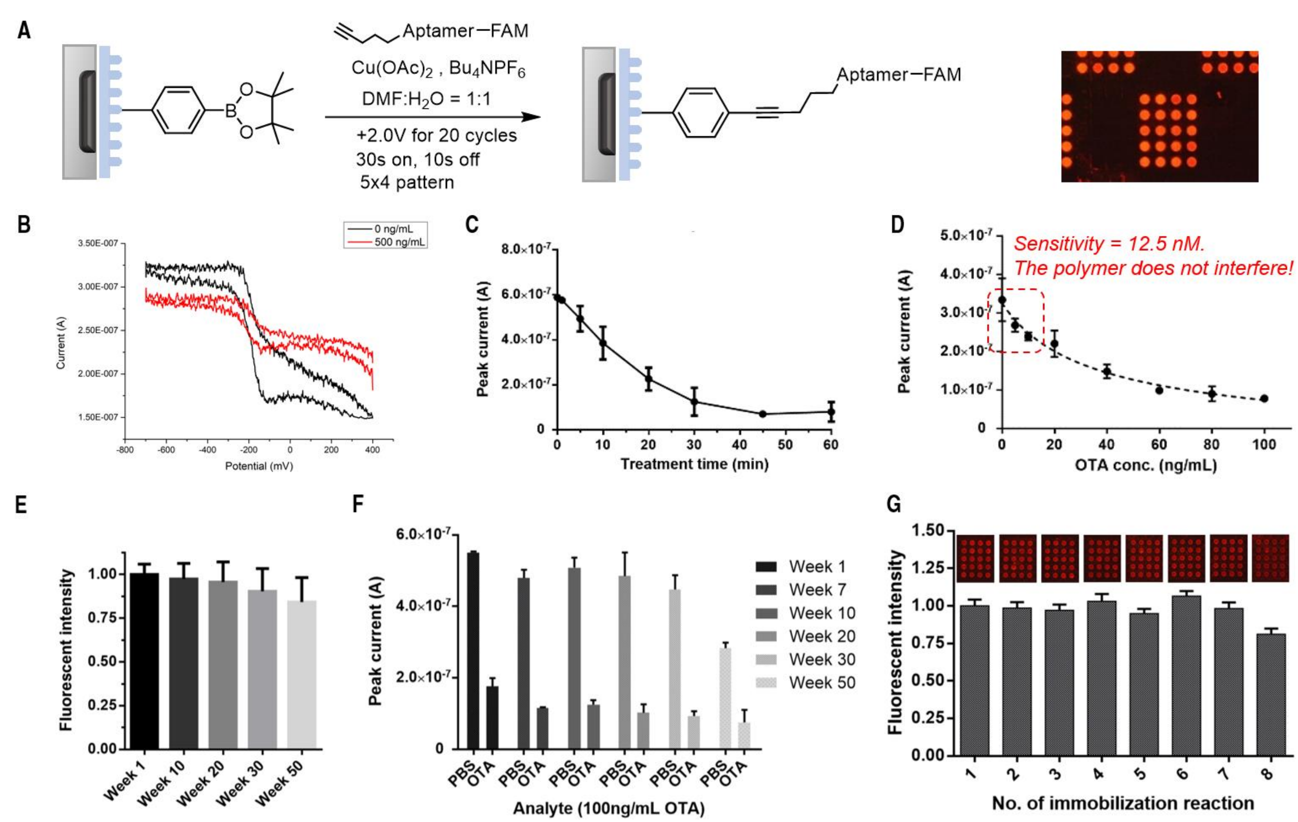

Figure 3. An initial test of the diblock copolymer surface with a known ochratoxin A/aptamer pair. (**A**) Chan-Lam coupling reaction for placing the aptamer on the array. (**B**) CV study for ochratoxin A/aptamer pair. The black line shows the CV for the hydroquinone/quinone redox mediator (8 mM in PBS) in the absence of OTA. The red line shows the CV for the same redox pair following the addition of 500 ng/mL of OTA to the solution above the array. (**C**) A check of signaling response time. The functionalized array was treated with a solution containing 500 ng/mL of OTA and then the peak current measured over time. (**D**) A calibration curve to determine the sensitivity of the experiment. In this case, the functionalized array was treated with varying concentrations of OTA and the peak current monitored after 30 min. (**E-F**) Long-term storage stability test for the polymer coated array. (E) Monitoring surface stability using fluorescence for the OTA-aptamer functionalized array over a year. (F) Monitoring the compatibility of the array with signaling studies for that year period. (**G**) Probing the stability of a functionalized array surface to multiple Chan-Lam coupling reactions.

of the two processes, the distance that the Cu(II) can migrate from the electrode of its origin can be manipulated so that the desired Chan-Lam coupling reaction can only happen at the selected electrodes. As part of balancing the rate of Cu(II) generation at the electrode and its consumption in solution, the electrodes selected for the oxidative generation of Cu(II) were cycled on and off. This slowed the generation of Cu(II) at the electrode so that the solution phase reduction of Cu(II) could keep pace. The success of the strategy was assessed by placing a fluorescent label onto the surface of the selected electrodes and then examining the array with a fluorescence microscope.

The question we wanted to answer with this project was whether this approach to the surface on a microelectrode array might provide the alternative, stable platform needed to begin building the "point-of-care" diagnostic devices proposed in Figure 1. Four key questions needed to be addressed in order to take this step. First, would the Chan-Lam coupling reaction work with larger molecules like a DNA aptamer, and was the method compatible with the total synthesis of a complex addressable surface using the larger molecules? Second, was the polymer coating compatible with the indirect method of detecting aptamer binding proposed and did it lead to the sensitivity needed to detect a metabolite in urine? Third, did the new surface really have the stability needed for a point-of-care device, and fourth, was the approach compatible with the multiplex detection of more than one metabolite at a time?

To answer these questions and validate the performance of the surface, the use of a well-established, commercially available aptamer targeting ochratoxin A was selected (Figure S1).[23] The aptamer was purchased with an acetylene on one end for the Chan-Lam coupling reaction and a fluorophore on the other for evaluating the success of that reaction. To this end, placement of the aptamer on an array proceeded exactly as planned, and its success can be seen in the fluorescence image provided (Figure 3A). Blocks of 20 electrodes each were selected for the placement reaction that employed the reaction conditions shown in Figure 2C along with a solution phase aptamer concentration of 100 μM. The method led to the placement of DNA on the electrodes with a density of around 177 pmol/cm^2 (please see the supporting information). This very high level of surface density is the result of two features of the current approach. First, the Chan-Lam coupling reaction is very efficient and converts a high percentage of the arylborate groups on the surface of the electrode to the cross-coupling product. Second, the porous polymer surface provides a high number of reaction-accessible sites on the electrode surface. In the end, the initially developed array-based synthetic method was robust enough to accommodate the large change in structure from a small molecule to the DNA oligomer.

The modified microelectrode array was then examined for its response to the presence of ochratoxin A. To this end, it was submerged in an 8mM solution of quinone/hydroquinone in PBS buffer. The black cyclic voltammetry (CV) curve (Figure 3B) was taken for the redox mediator. To this mixture was added 500 ng/mL of ochratoxin A, a change that led to the red CV curve for the redox pair and evidence that the polymer supported aptamer still bound effectively to its target.

Two experiments were then attempted (Figure 3, C and D). In the first, an array functionalized with the aptamer was treated with an electrolyte solution containing 500 ng/mL of ochratoxin A and the drop in current associated with the binding event monitored over time. Each data point in the graph represents the average current for four blocks of 20 electrodes with the current for each block being the sum of the currents measured at each individual electrode. In the experiment, a change in current could be detected almost immediately, but the maximum signal was not observed for 30 minutes. Due to this response time, in all subsequent signaling experiments the current was recorded 30 minutes following the addition of a metabolite to the solution above the array. The 30 minute delay in obtaining the maximum signal appears to be the result of a slow equilibration of the polymer in response to the binding event on its surface. The current measured at an electrode in the array reflects the amount of mediator at its surface, a quantity that is dependent on the equilibrium concentration of the mediator in the polymer. This concentration is determined by the rate of diffusion of the mediator within the polymer. A change on the surface of the polymer alters this dynamic by altering the structure of the polymer and changing the rate of diffusion for the mediator within that structure. Time is then required to reestablish an equilibrium concentration of the mediator within the polymer, and it is only after this equilibrium is fully established that the maximum signal change for the binding event is observed. In the future, efforts to minimize this delay will focus on the use of a thinner, more porous polymer that allows faster diffusion to the electrode surface below.

In the second experiment, the functionalized array was treated with varying concentrations of ochratoxin A (OTA) to generate a calibration curve for the interaction. Of note, the presence of OTA in solution could be detected at a concentration of 12.5 nM, a value consistent with that of other detection methods.[23] So while use of the polymer coating did lead to a slower response time, it did not interfere with the sensitivity of the experiment. This was especially important because the clinically relevant limit of detection (LOD) for OTA in urine falls within the micromolar range. This clinically relevant limit of detection is consistent with the value typically needed for identifying other metabolites in urine as well. So, the polymer coated electrodes do have the sensitivity needed for the proposed application.

Stability: Attention was then turned to whether the polymer coated electrode had the stability needed for a "point-of-care" device (Figure 3, E and F). An array was prepared with multiple blocks of 20 electrodes functionalized with the OTA-aptamer. The array was then examined using a fluorescence microscope and the intensity of the signal from the array recorded (Figure 3E, week one). An electrochemical signaling study was then

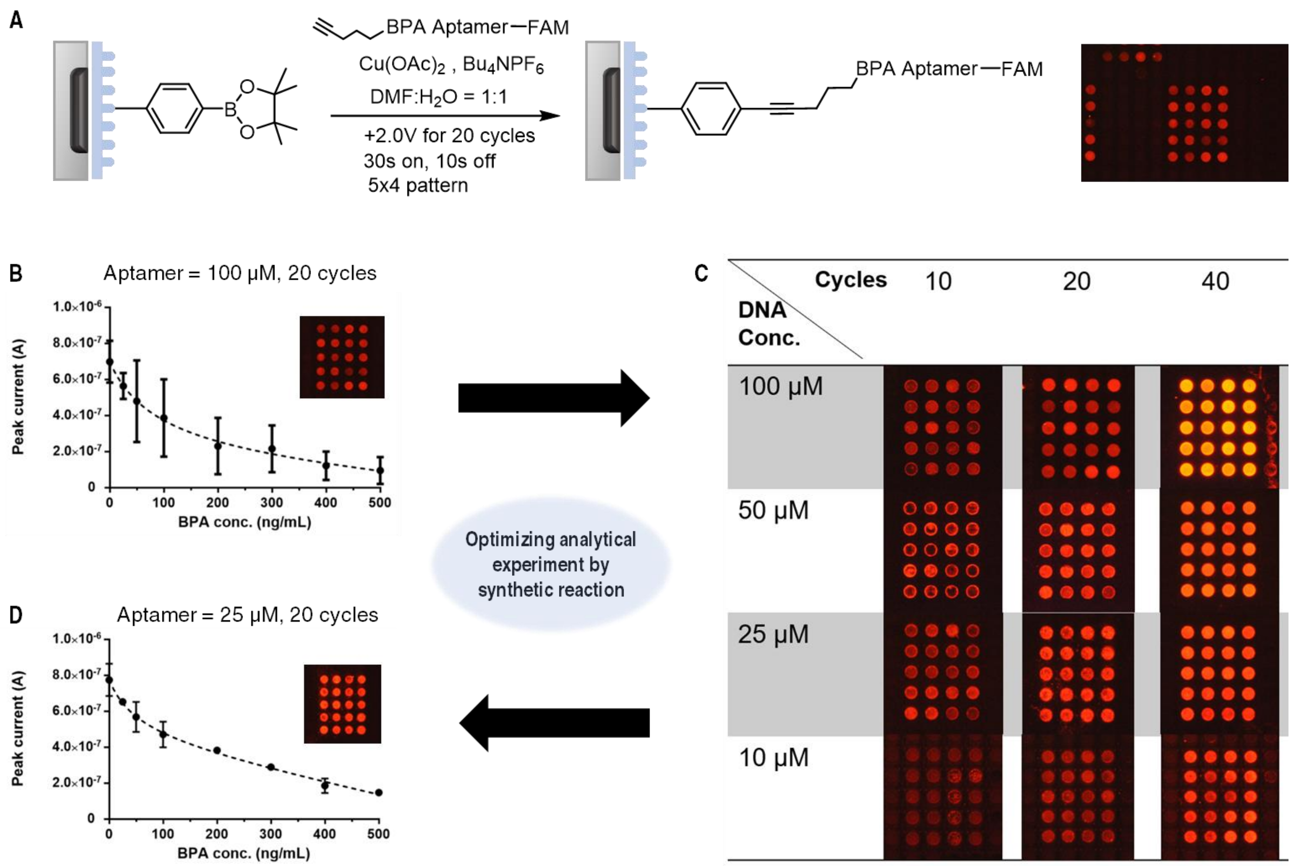

Figure 4. Studies of the diblock copolymer surface with a known BPA/aptamer pair. (**A**) Initial synthetic method to place a BPA-aptamer onto a 12K-array. (**B-D**) Optimization of the synthetic methodology and in so doing the subsequent signaling experiment.

conducted by comparing the current associated with the hydroquinone/quinone redox pair in a PBS buffer solution to the current for the same pair in a buffer solution containing 500 ng/mL of ochratoxin A. The presence of the ochratoxin A caused a significant drop in current at all of the electrodes where the aptamer was located. This data was recorded as week one in Figure 3F. The plotted data represents the average over five blocks of the electrodes and the error bars shown represent the spread in the data at those different sites on the array. The array was then washed and stored for 10 weeks in a plastic box placed in a drawer, without additional precautions. The experiments were then repeated (week 10 in the Figures). The fluorescence data indicated that the surface of the array did not change during storage, and the signaling data obtained remained the same as well. The array was then washed, stored for another 10 weeks, and then both the fluorescence and signaling study repeated again. This cycle was repeated for a total of 50 weeks. In the end, there was a slight loss of aptamer from the surface of the electrodes over the course of the study, and after 30 weeks and multiple uses the array did begin to suffer from a loss in the total current measured at the electrodes. After 50 weeks, the baseline current (the current measured at the electrodes in the absence of OTA) was approximately 53% of the baseline current measured at the same electrodes before the year-long experiment was started. However, the drop in current at the electrodes due to the targeted binding event between the surface bound aptamer and OTA did not change. Both at the start of the experiment and after 50-weeks, binding of the aptamer to its OTA target caused an approximately 70% drop in the baseline current. Even after approximately one year, the presence of OTA was still easily detected.

The loss of baseline current on the array over the course of the study may well be due to the repeated experiments run on the surface of the array and not time. In the study, a single array was utilized, stored, and then reutilized many times, and we know that the stability of the diblock copolymer is not perfect when exposed to too many reactions. For example, consider the data presented in Figure 3G. A polymer coated array was specifically tested for the stability of the polymer to multiple synthetic experiments. This was done by conducting eight consecutive Chan-Lam coupling reactions to place a fluorescently labeled OTA-aptamer on the array. After each experiment, the fluorescence associated with the new surface bound aptamer was measured. After the eighth reaction, a small amount of the fluorescence from the aptamer was lost indicating that changes to the surface were beginning to occur. So, there is a limit to how many times a polymer coated array can be used before alteration of the surface becomes a concern.

Of course, the exposure to multiple reactions or multiple analytical experiments over time is not something a point-of-care device needs to endure. Such devices are stored over time and then used once. It is clear that the use of a diblock copolymer surface on the array provides more than enough stability for those applications.

Multiplex Detection: The next critical step was determining if the approach is compatible with the detection of more than one metabolite at a time. With that, attention was turned toward determining the generality of the chemistry developed for the OTA-based study. The issue was initially addressed with the use of an aptamer targeting bisphenol A (BPA). [24] The BPA-aptamer was 21 bases longer (63 vs. 42) than the OTA-aptamer (Table S1). Initially, the exact same strategy highlighted in Figure 3 was used to place the BPA-aptamer on a polymer coated 12K-array. The success of the experiment is shown in the Figure 4A. The reaction was nicely confined to the selected electrodes, however, the fluorescence image showed an uneven coverage of those electrodes.

This uneven coverage proved problematic as it led to large error bars in the subsequent signaling experiment (Figure 4B). The experiment was conducted in the exact same manner as the previous study shown in Figure 3D with each point representing the average current measured at 4 separate blocks of 20 electrodes each. Once again, the current used for each block of electrodes was the sum of the current measured at each of the 20 electrodes. In this case, the error in the data obtained from various sites on the array was so large that it rendered the binding curve questionable at best. This indicates that the variation in electrode coverage obtained from the Chan-Lam coupling reaction was not just within a block of electrodes, but also from one site on the array to another.

While initially worrisome, the array-based Chan-Lam coupling reaction is a synthetic method that can be optimized. Like all synthetic methods, the quality of the reaction depends on reaction time and the concentration of the substrates in solution. In Figure 4C, a series of optimization experiments is highlighted. The number of cycles used (horizontal axis) controls the time allowed for the synthetic method with each cycle having the selected electrodes turned on for 30 seconds and then off again for 10 seconds. A reaction run for 40 cycles had the electrodes turned on for a total of 20 minutes. The concentration of the substrate used (vertical axis) was also varied. For this study, it is important to remember that the excess substrate in the solution above the array also serves as the confinement strategy for the reactions (Figure 2B). Therefore, the presence of too much substrate will suppress the reaction on the surface of the electrodes. It is a balance between the amount of active reagent generated (maximized as one moves to the right in the Figure) at the electrodes and the consumption of that reagent in the solution above the array (maximized as one moves up in the Figure) that leads to optimization of the reaction. In this case, a longer reaction time and reduced confinement reaction led to optimal surface coverage. This result was consistent with a lower reactivity of the BPA-aptamer presumably due to its larger size and different secondary structure which would impact accessibility to the surface. The longer reaction time and reduced confinement reaction compensated for this slower reaction. Notably, the synthetic method could be modified to accommodate this change. For the BPA aptamer, the best balance between reaction time and surface coverage of the electrodes was found to be a reaction run for 20 cycles with an aptamer concentration in solution of 25 μM.

When an array functionalized with the BPA-aptamer using these reaction conditions was employed in a signaling study, the binding curve generated showed significantly reduced error. *Clearly, the quality of the signaling experiment was directly controlled by the quality of the synthetic reaction used to functionalize the polymer surface on the array.*

At this point, an aptamer for the antibiotic chloramphenicol (Cam) was also added to the array.[25] The Cam-aptamer has a molecular weight roughly the same as that of the OTA-aptamer (Table S1). Placement of the Cam-aptamer on the array (Figure 5A) proceeded nicely using the same optimized conditions employed for the OTA-aptamer (Figure S4) and not as well using the optimized conditions for the larger BPA-aptamer (20 cycles with an aptamer concentration of 25 μM). Once the aptamer was placed onto the array, the signaling study was conducted by varying the concentration of Cam in the solution above the array and monitoring the peak current associated with the hydroquinone/quinone redox pair. While the current drop-off in this case was less than observed for the OTA- and BPA-aptamers, the error bars were significantly smaller than the total drop in current, a scenario that allowed for easy detection of the binding event.

With the data for the three individual aptamers in place, a single array was functionalized with all three aptamers by placing each aptamer by 12 blocks of 20 electrodes each. Another 12 blocks of 20 electrodes each was used as a control. In total, the subsequent signaling studies summarized in Figure 5B utilized 960 microelectrodes in the array. In the Figure 5C-E each set of aptamer functionalized electrodes is shown and its response to a series of different analytes in solution recorded. The analytes were used in a concentration of 100 ng/mL, a concentration known to lead to maximum binding with the surface bound aptamers. In each example, the array was treated with PBS, the small molecule target for the aptamer, a mixture of OTA, BPA, and Cam, and then a solution with the two small molecules not recognized by the aptamer. For example, the experiment shown on the upper left in the Figure highlights the electrodes in the array functionalized with the OTA-aptamer. The error bars reflect the spread in the data over the 4-blocks of 20 electrodes used for each measurement. The data on the left of the OTA-aptamer experiment was the background recorded for the PBS buffer negative control, the data

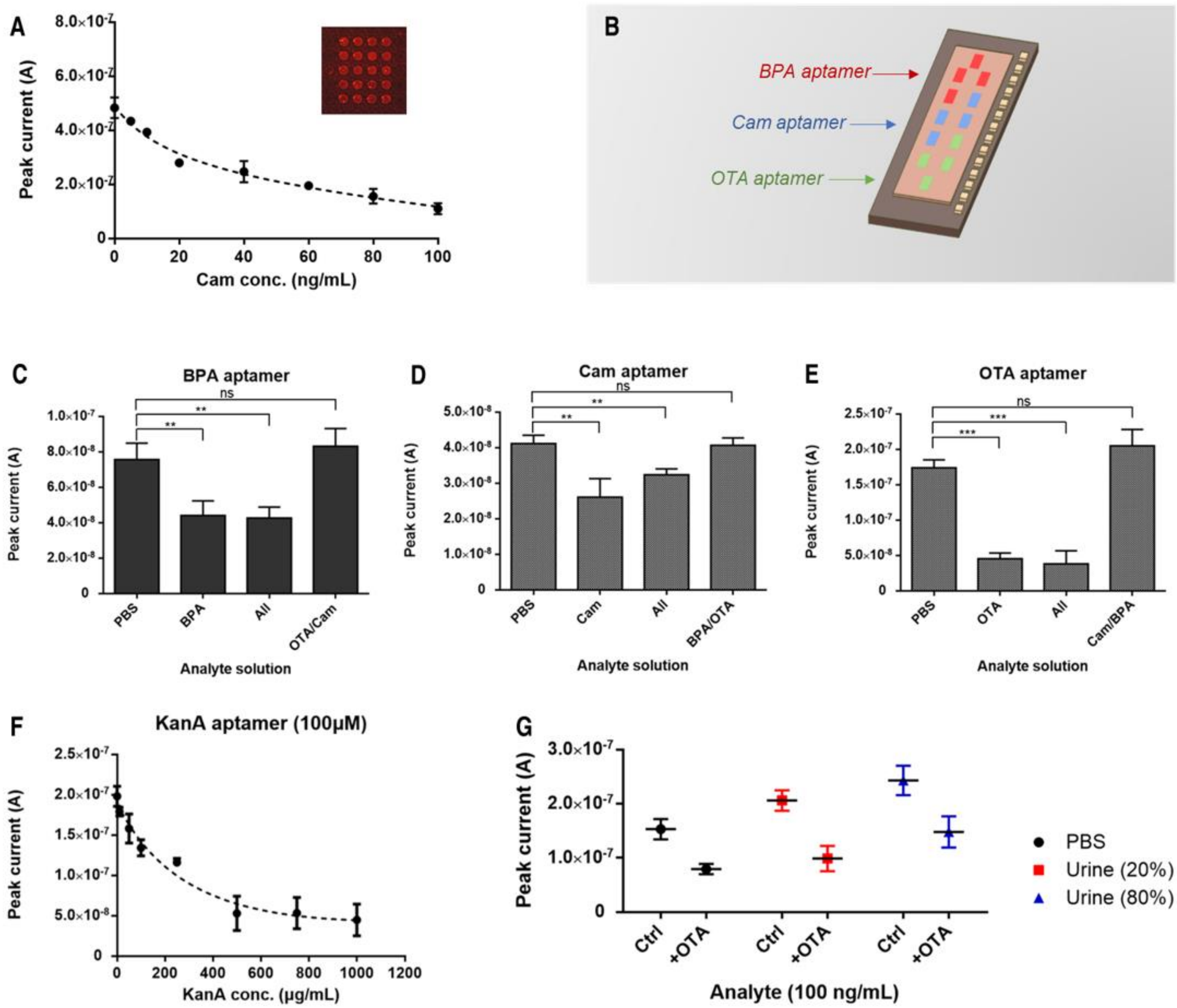

Figure 5. Multiplex sensing and toward point-of-care applications. (**A**) Data for the Cam/Cam-aptamer combination. (**B-E**) Multiplex sensing on a high-density microelectrode array. All three sensing experiments were conducted on a single array functionalized with the three aptamers. (**F**) The electrochemical signal associated with a KanA-aptamer/KanA pair. (**G**) A test of signaling compatibility with a single urine sample.

second to the left shows the drop in current at the OTA-aptamer functionalized electrodes when the array was treated with OTA, the third set of data shows the drop in current at the OTA functionalized electrodes when the array was treated with a mixture of all three small molecules, and finally the data on the right shows the current obtained at the OTA-aptamer functionalized electrodes when the array was treated with a mixture of BPA and Cam. The data definitively shows that the OTA-aptamer functionalized electrodes exclusively recognize OTA even when that OTA is part of a mixture of molecules. The current recorded at the OTA-aptamer functionalized electrodes is not altered by the other two small molecules. The current drop for the experiment with the OTA and for the experiment when all three small molecules were added to the array were the same as were the current measured for the negative control with just the PBS buffer and the current measured for the mixture of BPA and Cam without OTA. In the experiment, the OTA-aptamer functionalized electrodes were directly exposed to BPA and Cam both in the presence and absence of OTA. In every case, neither molecule either bound the OTA-aptamer or interfered with OTA binding the OTA-aptamer.

A similar experiment was conducted at the BPA- and Cam-functionalized electrodes (Figure 5D and 5E). In both cases, the result was the same. The current at the electrodes dropped when the array was treated with the matching small molecule (BPA or Cam) or a mixture of the three small molecules but not when treated with the two molecules that did not match the aptamer on the electrode surface. In combination, the array could detect the presence of all three small molecules or any combination of the small molecules. A mixture of OTA and Cam for example would signal at the OTA- and Cam-aptamer functionalized electrodes and not the BPA-aptamer functionalized sites, etc.

The use of a diblock copolymer coated, high density microelectrode array provides a platform that is stable for a year and enables the multiplex detection of small molecule targets!

Unpacking the Role of Aptamer Structure in Electrochemical Signaling: While the multiplex experiment worked fine, comparing the aptamer-target interactions side by side did highlight the relatively small change in current associated with the Cam-aptamer/Cam pairing, a change that was also reflected in the solo data shown in Figure 5A. The differences in the current change were not due to difference in the affinity of the small molecules and their associated aptamers. The binding of OTA to the OTA-aptamer used is 0.36 μM,[26] BPA for the BPA-aptamer used 8.3 nM,[24] and Cam for the Cam-aptamer used 0.77 μM.[27] Certainly, these numbers would not give rise to the largest current drop for the OTA/OTA-aptamer pair. Instead, it is important to note that we tend to think of aptamers in their extended "cartoon" picture in the absence of a ligand and then folded compactly only when the aptamer binds the ligand. However, for many aptamers this picture is not real. Single stranded DNA aptamers are able to form numerous intrastrand base pairing interactions, causing them to adopt stable folded structures even in the absence of ligand. The extent to which presence of the ligand causes a change in the structure and volume of the folded aptamer is then highly variable between different sequences. On an array, when this change in structure is more subtle, the result would be only a small change on the surface of an array and only a small current change. This appears to be the case for the Cam-aptamer.

In support of this suggestion, a kanamycin A (KanA)-aptamer developed by the Heemstra group specifically for its structure switching ability was examined on a microelectrode array for its binding to KanA.[28] The aptamer was labeled with an acetylene and a fluorescent tag in a manner identical to the OTA, BPA, and Cam-aptamers used above (Figure S4), and then it was placed by blocks of 20 electrodes each on a 12K-microelectrode array in a manner identical to that shown in Figure 2C (20 cycles for the reaction time and a substrate concentration of 100 μM). The array was then treated with various concentrations of KanA in the presence of the hydroquinone/quinone redox pair and the peak current for the redox pair recorded as a function of concentration (Figure 5F). In this experiment, the current drop matched that observed for the earlier OTA-aptamer/OTA pair. This observation was consistent with both the OTA-aptamer being selected to undergo a large structure switch upon binding OTA and our hypothesis the size of the current measured on an array directly reflects the degree to which an aptamer undergoes this change. For the future development of a point-of-care device, it appears that aptamers should be selected not only for their ability to bind a target ligand, but also for the extent to which their structure switches because of that event.[29]

Assessing Electrochemical Responses in Urine Medium for Point-of-Care Device Development: While the proof-of-principle studies shown above provide evidence that the method has the stability and multiplex detection capabilities needed for a point-of-care device, those studies are only good if the surface is also compatible with urine samples, the medium in which many metabolites are found. In principle, this should not be a problem. The diblock copolymer is stable to the pH's one would find in a typical urine sample, and the electrochemical study measures total current. Hence, electrolytes, catechols, and other moieties that oxidize in the same place as hydroquinone would only add to the total current. The change in surface induced by the binding of an aptamer to its ligand would alter that total current in the same way. This does appear to be the case. In Figure 5G, a single urine sample is examined both with and without added OTA (100 ng/mL for all three cases). Note how the current increases as the percentage of urine used to synthesize the sample increases. The addition of OTA then causes the same decrease in that total current.

Of course, urine samples can vary greatly (electrolyte concentration, the presence of mucin, etc.), and an examination of a single sample that does not account for gender, ethnicity, age, etc., does not in any way establish the broad compatibility of the method with urine samples. What the experiment does show is that if the urine sample does not interfere with binding of the aptamer to its target, then the use of a diblock copolymer surface and an indirect electrochemical method for monitoring current do allow for the detection of that interaction. Hence, the work here sets the stage for a more intensive investigation.

Conclusions:

The use of a diblock copolymer coating on a microelectrode array allows for the state-of-the-art detection of metabolites using aptamer-based electrochemical sensors to be extended from the detection of a single metabolite with a surface that is stable for under a month to the multiplex detection of metabolites on a surface that is stable for a year or more. While there was a need for optimization of the original Chan-Lam coupling reaction for larger DNA oligomers, the method was compatible with the construction of complex surfaces on the array with an example provided here of an experiment that capitalized on 960 electrodes in a high-density array. While the electroanalytical experiment had a slower response time of approximately 30 min, the sensitivity of the experiment was not altered by the use of the diblock copolymer surface. The detection limit of the analytical system and the overall stability of the surface are fully consistent with the detection of metabolite samples in urine medium where they are typically found in micromolar concentrations. Studies to examine the broad compatibility of the experiments in urine medium are underway.

In the end, the use of the diblock copolymer coating on a microelectrode array can potentially enable translation of the initial intriguing demonstrations that electrochemical methods can be used for metabolite detection into a practical point-of-care device. Note that in meeting this challenge, the chemistry that has been developed is not restricted to the use of an aptamer or any one method of recognition. The reactions and the surface are compatible with oxidation reactions, reduction reactions, acid and base reactions, Lewis acid catalysis, transition metal cross-coupling reactions, Diels-Alder reactions, click-reactions, and more.[21] So, many different types of recognition elements from proteins to aptamers, can in principle be placed on the same array.

ASSOCIATED CONTENT

Supporting Information

Sample experimental procedures for the site-selective reactions are included along with procedures for the cyclic voltammetry studies. This material is available free of charge via the Internet at http://pubs.acs.org."

Data Availability

All data underlying this study are available in the published article and its online supplementary material.

AUTHOR INFORMATION

Corresponding Authors

Kevin D. Moeller: moeller@wustl.edu

Notes

The authors declare no competing financial interests.

Acknowledgement: We thank the National Science Foundation (Center for Synthetic Organic Electrochemistry: CHE-2002158) and the National Institutes of Health (1R01 GM122747) for supporting the work that provided the foundation for this effort and (R35 GM144075) for supporting development of the KanA aptamer.

References

1. Larsson, D. G. J.; Flach, C. F., Antibiotic Resistance in the Environment. *Nat. Rev. Microbiol.* **2022**, *20*, 257-269.
2. Aminov, R. I., The Role of Antibiotics and antibiotic Resistance in Nature. *Environ. Microbiol.* **2009**, *11(12),* 2970-2988.
3. Boucher, H. W., Bad Bugs, No Drugs 2002-2020: Progress, Challenges, and Call to Action. *Trans. Am. Clin. Climatol Assoc.* **2020**, *131*, 65-71.
4. Karbelkar, A. A.; Furst, A. L. Electrochemical Diagnostics for Bacterial Infectious Diseases. *ACS Infect. Dis.* **2020**, *6*, 1567-1571. Doi:10.1021/acsinfecdis.0c00342
5. Simoska, O.; Stevenson, K. J. Electrochemical Sensors for Rapid Diagnosis of Pathogens in Real Time. *Analyst* **2019**, *144*, 6461-6478. doi: 10.1039/c9an01747j
6. Chandra, S.; Siraj, S.; Wong, D. K. Y. Recent Advances in Biosensing for Neurotransmitters and Disease Biomarkers using Microelectrodes. *ChemElectroChem*, **2017**, *4*, 822-833. doi:10.1002/celc.20160081
7. Kell, D. B.; Brown, M.; Davey, H. M.; Dunn, W. B.; Spasic, I.; Oliver, S. G. Metabolic Footprinting and Systems Biology: The Medium is the Message. *Nat. Rev. Microbiol.* **2005**, *3*, 557-565. doi: 10.1038/nrmicro1177.
8. Cambau, E.; Poljak, M. Sniffing Animals as a Diagnostic Tool in Infectious Diseases. *Clon. MIcrobiol. Infect.* **2020**, *26*, 431-435. doi: 10.1016/j.cmi.2019.10.036.
9. Scott-Thomas, A. J.; Syhre, M.; Pattemore, P. K.; Epton, M.; Laing, R.; Perason, J.; Chambers, S. T. 2-Aminoacetophenone as a Potential Breath Biomarker for Pseudomonas Aeruginosa in the Cystic Fibrosis Lung. *BMC Pulm. Med.* **2010**, *10*, 56. doi: 10.1186/1471-2466-10-56.
10. Quinn, L.; Ailsworth, M.; Matthews, E.; Kellams, A.; Shirley, D. –A. Serratia Marcescens Colonization Causing Pink Breast Milk and Pink Diapers: A Case Report and Literature Review. *Breastfeed Med.* **2018**, *13*, 388-394. doi: 10.1089/bfm.2018.0002.
11. Slinker, J. D.; Muren, N. B.; Gorodetsky, A. A.; Barton, J. K., Multiplexed DNA-Modified Electrodes. *J. Am. Chem. Soc.* **2010,** *132* (8), 2769-2774.
12. Furst, A. L.; Smith, M. J.; Francis, M. B Direct Electrochemical Bioconjugation on Metal Surfaces. *J. Am. Chem. Soc.* 2017, *139*, 36, 12610–12616. doi: 10.1021/jacs.7b06385
13. Downs, A. M.; Plaxco, K. W., Real-Time, *In Vivo* Molecular Monitoring Using Electrochemical Aptamer Based Sensors: Opportunities and Challenges. *ACS Sens.* **2022**, *7*, 2823-2832 and references therein.
14. Zhou, X.; Zamani, M.; Austin K.; De Bock, M.; Ullola, J. C.; Riki, S.; Furst, A. L. *Chem. Commun.* **2024**, *60*, 1948-1951.
15. Love, J. C.; Estroff, L. A.; Kriebel, J. K.; Nuzzo, R. G.; Whitesides, G. M., Self-Assembled Monolayers of Thiolates on Metals as a Form of Nanotechnology. *Chem Rev.* **2005,** *105* (4), 1103-1170.
16. Strulson, M. K.; Johnson, D. W.; Maurer, J. A. Increased Stability of Glycol-Terminated Self-Assembled Monolayers for Long-Term Patterned Cell Culture. *Langmuir*, **2012**, *28*, 4318. doi: 10.1021/la2035533.
17. Chen, N.; Li, S.; Zhao, P.; Liu, R.; Xie, Y.; Lin, J.-L.; Nijhuis, C. A.; Xu, B.; Zhang, L.; Xu, H.; Li, Y., Extreme long-lifetime self-assembled monolayer for air-stable molecular junctions. *Sci Adv.* **2023,** *9* (42), eadh3412.
18. Hu, L.; Bartels, J. L.; Bartels, J. W.; Maurer, K.; Moeller, K. D., A New Porous Reaction Layer for Developing Addressable Molecular Libraries. *J. Am. Chem. Soc.* **2009,** *131* (46), 16638-16639.
19. Drayton-White, K.; Liu, S.; Chang, Y. C.; Uppal, S.; Moeller, K. D., Microelectrode arrays, electrosynthesis,

and the optimization of signaling on an inert, stable surface. *Beilstein J Org Chem* **2022,** *18*, 1488-1498.

20. Graaf, M. D.; Moeller, K. D. An Introduction to Microelectrode Arrays, The Site-Selective Functionalization of Electrode Surfaces, and the Real-Time Detection of Binding-Events. *Langmuir* **2015**, *31*, 7697-7706. DOI: 10.1021/la504254e.
21. Kruger, R.; Moeller, K. D. Capitalizing on Mediated Electrolyses for the Construction of Complex, Addressable Molecular Surfaces. *J. Org. Chem.* **2021**, *86*, 15487-15865. DOI: 10.1021/acs.joc.1c01609.
22. Huang, A.; Krueger, R.; Moeller, K. D. Microelectrode Arrays, Electrocatalysis, and the Need for Proper Characterization. *ChemElectroChem* **2023**, e202300457. DOI: 10.1002/celc.202300457.
23. Chen, J.; Fang, Z.; Liu, J.; Zeng, L., A simple and rapid biosensor for ochratoxin A based on a structure-switching signaling aptamer. *Food Control* **2012,** *25* (2), 555-560.
24. Jo, M.; Ahn, J. Y.; Lee, J.; Lee, S.; Hong, S. W.; Yoo, J. W.; Kang, J.; Dua, P.; Lee, D. K.; Hong, S.; Kim, S., Development of single-stranded DNA aptamers for specific Bisphenol a detection. *Oligonucleotides* **2011,** *21* (2), 85-91.
25. The CAM-aptamer can be purchased from Integrated DNA Technologies, 1710 Commercial Park, Coralville, IA 52241-2760, Ref. Number 426396525. Purification: Standard Desalting; Modifications: 5' Hexynyl, 3' 6-FAM.
26. Cruz-Aguado, J. A.; Penner, G. Determination of Ochratoxin A with a DNA-Aptamer. *J. Agric. Food Chem.* **2008**, *56*, 10456-10461.
27. Mehta, J.; Van Dorst, B.; Rough-Martin, E.; Herrebout, W.; Scippo, M. –L.; Blust, R.; Robbens, J. *In Vitro* Selectrion and Characterization of DNA-Aptamers Recognizing Chloramphenicol. *J. Biotech.* **2011**, *155*, 361-369.
28. Sanford, A. A.; Rangel, A. E.; Feagin, T. A.; Lowery, R. G.; Argueta-Gonzalez, H. S.; Heemstra, J. M., RE-SELEX: restriction enzyme-based evolution of structure-switching aptamer biosensors. *Chem Sci.* **2021,** *12* (35), 11692-11702.
29. Wu, Y.; Ranallo, S.; Del Grosso, E.; Chamoro-Garcia, A.; Ennis, H. L.; Milosavić, N.; Yang, K.; Kippin, T.;Ricci, R.; Stojonavic, M.; Plaxco, K. W., Using Spectroscopy to Guide the Adaptation of Aptamers into Electrochemical Aptamer-Based Sensors. *Bioconjug. Chem.* **2023,** *34*(1),124-132.

Table of Content graphic